

Suppression effect on the Berezinskii–Kosterlitz–Thouless transition in growing networks

S. M. Oh¹, S.-W. Son^{2,3}, and B. Kahng¹

¹*CCSS, CTP and Department of Physics and Astronomy, Seoul National University, Seoul 08826, Korea,*

²*Department of Applied Physics, Hanyang University, Ansan 15588, Korea,*

³*Asia Pacific Center for Theoretical Physics, Pohang 37673, Korea*

(Dated: June 7, 2022)

Growing networks are ubiquitous in the real world, ranging from coauthorship socio-networks to protein interaction bio-networks. The Berezinskii-Kosterlitz-Thouless (BKT) transition appears widely in the evolution of these systems. Here, we show that when the growth of large clusters is suppressed, the BKT transition can change to a first-order transition at a delayed transition point p_c . Moreover a second-order-type critical behavior appears in a wide region of the link occupation probability before the system explodes, in which while the largest cluster has not grown to the extensive size of the system yet, the mean cluster size diverges. Far below p_c , the property of the infinite-order transition still remains. Accordingly, the features of infinite-order, second-order, and first-order transitions all occur in a single framework when the BKT transition is suppressed. We present a simple argument to explain the underlying mechanisms of these abnormal transition behaviors.

I. INTRODUCTION

Berezinskii, Kosterlitz and Thouless (BKT) discovered an infinite-order topological phase transition in early 1970s [1–7]. Since then, its notion has been widely used for understanding diverse phenomena ranging from the superfluid-normal phase transition [6] and quantum phase transitions [7] in physical systems to percolation transitions (PTs) of growing networks [8, 9] in interdisciplinary areas.

Growing networks are ubiquitous in the real world. Some examples are coauthorship networks [10, 11], the World Wide Web (WWW) [12], and protein interaction networks [13–15]. In growing networks, the number of nodes increases with time. The coauthorship network [10, 11] is growing as a new graduate student writes the first paper with other colleagues. The WWW is growing as a new page is created and the protein interaction network is growing by a gene mutant. We recall a simple growing model introduced by Callaway et al. [8], called the growing random network (GRN) model hereafter. A node, representing a person, a web page, or a protein, is present in the system at the beginning. At each time step, a node is added. A link is also added with probability p between a pair of unconnected nodes chosen randomly among all existing nodes. As p is increased, a PT occurs at a transition point p_c , beyond which a macroscopic-scale large cluster is generated. A cluster represents social community, hyperlinked web pages, or protein complexes binding together.

Following the basic idea of Paul Ehrenfest in 1933 [16], phase transitions are normally classified by the lowest derivative of the free energy that is discontinuous at a transition point. First-order phase transitions exhibit a discontinuity in the order parameter and finite fluctuations, and second-order phase transitions are continuous in the first derivative (the order parameter), but diverges in the second derivative such as the susceptibility at a

transition point. The latter transition has also features that the correlation length diverges and the correlation function decays in a power-law manner at the transition point. Under this classification scheme, there could in principle be higher-order phase transitions. Actually, it was revealed that the PT of the GRN model follows an infinite-order BKT transition [8]. The order parameter, the relative giant cluster size, $G(p)$ is zero for $p < p_c$ and increases continuously for $p > p_c$ in the essentially singular form

$$G(p) \sim \exp(-a/\sqrt{p-p_c}), \quad (1)$$

where a is a positive constant. Thus, the PT is infinite-order. In this case, the cluster size distribution $n_s(p)$ follows a power law $n_s \sim s^{-\tau}$ without any exponential cutoff in the entire region of $p < p_c$ [8, 9, 15, 17]. Thus, the region $p < p_c$ is often referred to as the critical region. The exponent τ decreases with increasing p and approaches $\tau = 3$ as $p \rightarrow p_c$ from below [9, 15]. Thus, the mean cluster size, $\sum_s s^2 n_s$, is finite for $p \leq p_c$. Moreover, for $p > p_c$, $n_s(p)$ of finite clusters decays exponentially. Thus, $\sum_s s^2 n_s(p)$ is finite. The behaviors of the order parameter and the mean cluster size are depicted schematically in Figs. 1(a) and 1(b), respectively. These properties of a PT of growing networks are different from those of a second-order PT of static networks [18, 19].

In statistical physics, it is well known that a phase transition can be changed by long-range interaction. For instance, a PT in one dimension is changed to an infinite-order transition by $1/r^2$ long-range connections [20]. Similarly a PT can be changed by global suppression effect [21]. For instance, a second-order PT in two dimensions can be changed to a first-order one when formation of a spanning cluster is suppressed [22]. Here we remark that such PT-type changes due to long-range connection and global suppression effect were investigated only in the static case, in which the system size is fixed; however, it has never been investigated yet in growing networks. In

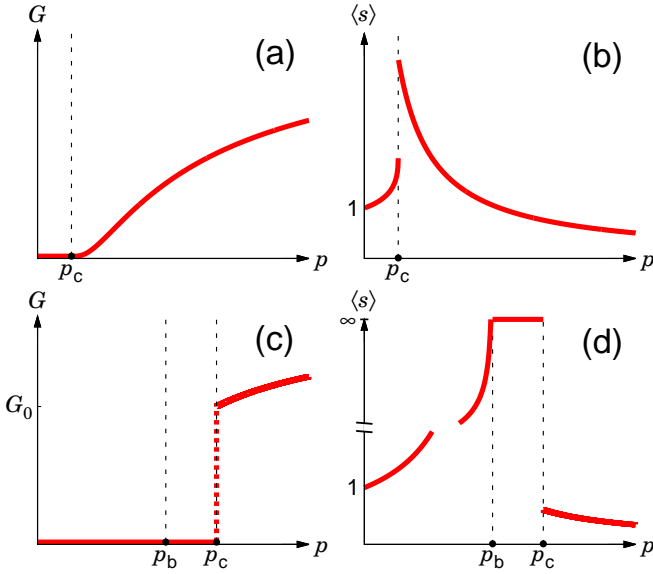


FIG. 1. Comparison of phase transitions between the infinite-order transition of the GRN model in (a) and (b) and the unconventional transition of the r -GRN model in (c) and (d). Plot of order parameter G versus p in (a) and (c). Plot of mean cluster size $\langle s \rangle$ versus p in (b) and (d).

this paper, we aim to investigate how the infinite-order PT is changed by a global suppression effect in growing networks.

Suppression dynamics may arise in growing networks, for instance, the coauthorship network [11]. As a new graduate student joins a group and writes a paper together with group members, the network is growing. As a research group becomes larger, the group can become more inefficient functionally in some aspect; thus, new students are less likely to join such a group and thus the growth of large groups can be suppressed. As new students join small or medium groups, those groups grow in size. Those large clusters can merge as postgraduates transfer to another large group, leading to an abrupt size increase of the largest cluster as we observed in the real-world data [11]. The evolution of such a coauthorship network does not proceed by purely random connections, but there can exist some suppression mechanism against the growth of large clusters. Moreover, the suppression effect can also arise in the WWW by inaccessibility.

Here, we investigate how the infinite-order PT of growing networks is changed by the suppression effect. To implement this, we modify the GRN model by including the suppression mechanism as follows: At each time step, a node is added to the system. To add a link, we select two nodes: a node from a portion of the smallest clusters and the other node from among all the nodes. They are connected with probability p . Because a node belonging to small clusters has twice the chance to be linked, while a node in large clusters has one chance, the growth of large clusters is suppressed. The dynamic rule becomes global in the process of sorting out the portion of the

smallest clusters among all cluster sizes. This model is called the restricted growing random network (r -GRN) model. This model is built based on the restricted Erdős-Rényi (r -ER) model [23–26], which is a static network. This model contains a global suppression dynamics and enabled us to obtain analytic solutions for various properties of a PT. Thus, we extend this model to growing networks. The detailed rule is presented schematically in Fig. 2 and will be described concretely in Sec. II.

Using the rate equation approach and performing numerical simulations, we find that the transition type of growing networks changes from an infinite-order to a first-order. A second-order critical behavior also occurs. Moreover, some characteristics of the infinite-order transition remains. Thus, those three phases emerge in a single model. The underlying mechanism is as follows: When the link occupation probability p is small and below p_c , most clusters are small and the suppression is not effective. Hence the infinite-order critical behavior of $n_s(p) \sim s^{-\tau(p)}$ appears as the one in the BKT transition. The exponent $\tau(p)$ decreases as p is increased. In the BKT transition, τ decreases down to three as p is increased; however, in this r -GRN model, the exponent $\tau(p)$ can decrease down to two, because the transition point is delayed by the suppression effect. On the other hand, if the cluster size distribution follows a power law without any exponential cutoff, the largest cluster size scales with the system size $N(t)$ in the steady state as $s_{\max} \sim N^{1/(\tau-1)}$. When τ decreases down to two, the largest cluster grows to the extent of the system size in the steady state. Therefore a discontinuous transition occurs.

As τ decreases below three, the mean cluster size, i.e., the susceptibility is no longer finite. We divide the region $p < p_c$ into two subregions, $p < p_b$ and $p_b < p < p_c$, such that for $p < p_b$, $\tau > 3$, whereas for $p_b < p < p_c$, $2 < \tau < 3$. Thus, the mean cluster size is finite and diverges in the former and latter regions, respectively. Therefore, another type of PT occurs at p_b . It is interesting to note that the mean cluster size diverges even though the giant cluster does not form yet in the interval $p_b < p < p_c$. That is because the cluster size distribution exhibits a critical behavior without an exponential cut-off. Large clusters still remain in the subextensive size, and they induce heavy fluctuations. We regard the region $p < p_b$ as an infinite-order critical region, because it is inherited from the infinite-order transition. The region $p_b < p < p_c$, in which a characteristic of the second-order transition appears, is regarded as the second-order critical region. At p_c , a first-order PT occurs. For $p > p_c$, the size distribution of finite clusters does not follow a power law. The region $p \geq p_c$ is regarded as a noncritical region. Thus, our model contains all the features of the infinite-order, second-order, and first-order transitions. The behaviors of the order parameter and the mean cluster size are depicted in Figs. 1(c) and 1(d), respectively. Therefore, when the infinite-order BKT transition is broken by the suppression effect, a first-order PT occurs; a

second-order critical phase appears; and an infinite-order critical phase still remains. We remark that this is the first observation of the first-order PT in random growing networks within our knowledge.

This paper is organized as follows: In Sec. II, we introduce a dynamic rule of the r -GRN model. In Sec. III, we set up the rate equation of the cluster size distribution as a function of link density p and time. In Sec. IV, the cluster size distribution is derived explicitly, and its implication is discussed. In Sec. V, the two critical points are determined using the generating function technique. In Sec. VI, the exponent $\tau(p)$ of the cluster size distribution is determined explicitly as a function of p in a limited case. We will discuss the implication of our results in the final Sec.

II. THE R -PERCOLATION MODEL OF GROWING NETWORKS

Let us begin with the introduction of r -GRN model. At the beginning, a system contains single node. At each time step, a node is added to the system. Thus, the total number of nodes at time step t becomes $N(t) = t + 1$. As time goes on, clusters of connected nodes form. We classify clusters into two sets, a set R and its complement set R^c , according to their sizes. Roughly speaking, the set R contains approximately gN nodes belonging to the smallest clusters, while the set R^c contains the nodes belonging to the rest large clusters. $g \in [0, 1]$ is a parameter that controls the size of R . Rigorously speaking, let c_i denote the i -th cluster in ascending size order. The set $R(t)$ contains the k smallest clusters, those satisfying $\sum_{i=1}^{k-1} s(c_i) < \lfloor gN \rfloor \leq \sum_{i=1}^k s(c_i)$, where $s(c_i)$ denotes the size of the cluster with index c_i . The complement set R^c contains the remaining (largest) clusters. Next, one node is selected randomly from the set $R(t)$ and another is selected from among all the nodes. Roughly speaking, a node in the set of smaller clusters has twice chance of being linked, while a node in the set of larger clusters has one chance. Then, a link is added between the two selected nodes with link occupation probability p . The dynamic rule becomes global in the process of sorting out the portion of the smallest clusters among all cluster sizes. Moreover, it suppresses the growth of large clusters by allowing less chance to be linked. This link connection process is visualized in Fig. 2 for the restricted fraction $g = 0.4$ as an example. This restriction rule is initially introduced in Ref. [24] and modified in Ref. [25, 26].

We define the size of the largest cluster in the set R as $S_R(p, t)$ for a given p at time t , which determines the size of the boundary cluster(s) between the two sets. It depends on the fraction g [25]. Thus, when $g = 1$, which means that S_R is equal to the size of the giant cluster $GN(t)$, this model reduces to the GRN model [8]. It has been found previously that the GRN model exhibits a continuous infinite-order phase transition at $p_c = 1/8$ [8].

However, when $g \rightarrow 0$, $S_R = 1$, and an isolated node in R

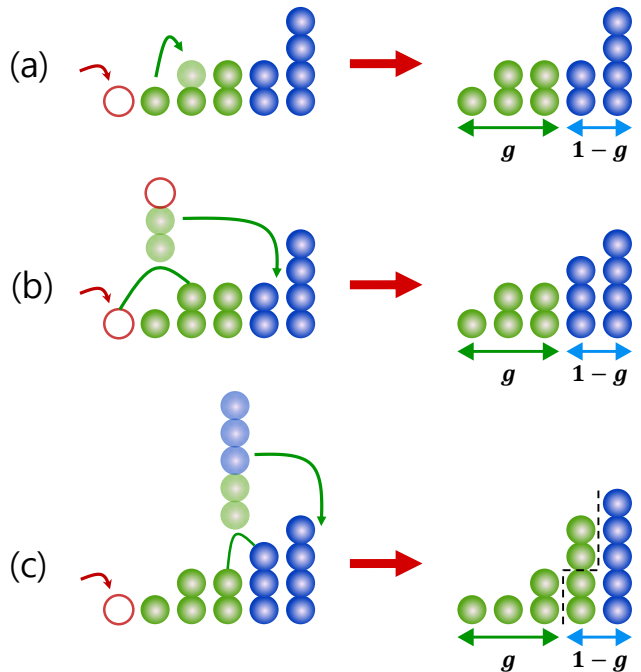


FIG. 2. Schematic illustration of the r -GRN model with $g = 0.4$. Nodes (represented by balls) in $R(t)$ are green (filled light gray), whereas those in $R^c(t)$ are blue (filled dark gray). Each column represents a cluster. In (a), the system contains five clusters with sizes (1, 1, 2, 2, 4), respectively, displayed from left to right. The leftmost red ball (open ball) is a node newly added to the system. The next three green clusters belong to the set R . The following two blue clusters belong to the set $R^c(t)$. After a node is added, the two nodes belonging to the first and second clusters in R are merged and become one cluster of size two. Then the total number of nodes N becomes 11, and S_R remains two. (b) In the next step after (a), a newly added node merges into the second cluster in R , generating a cluster of size three. This cluster moves to the set R^c . The set R contains three clusters and five nodes and has $S_R = 2$. The set R^c contains two clusters and seven nodes. (c) In the next step after (b), a new node is added. The third cluster in R and the first cluster in R^c merge and generate a cluster of size five that belongs to R^c . The cluster of size four in R^c at (b) moves to R . $S_R = 4$. Some nodes in the boundary cluster of size S_R are regarded as the elements of the set R .

and a node in R^c merge with link occupation probability p .

III. RATE EQUATION OF THE MODEL

Let us define the cluster number density $n_s(p, t)$ for a given p at time step t as the number of clusters of size s divided by the total number of nodes $N(t)$ at t . One can write the rate equations according to the relative magnitude of the cluster size from s to S_R for the cluster size distribution $N(t)n_s$ as follows:

$$\frac{d(N(t)n_s)}{dt} = p \left[\sum_{i,j=1}^{\infty} \frac{in_i j n_j}{g} \delta_{i+j,s} - \left(1 + \frac{1}{g}\right) s n_s \right] + \delta_{1s} \quad \text{for } s < S_R, \quad (2)$$

$$\frac{d(N(t)n_s)}{dt} = p \left[\sum_{i,j=1}^{\infty} \frac{in_i j n_j}{g} \delta_{i+j,s} - s n_s - \left(1 - \sum_{k=1}^{S_R-1} \frac{k n_k}{g}\right) \right] + \delta_{1s} \quad \text{for } s = S_R, \quad (3)$$

$$\frac{d(N(t)n_s)}{dt} = p \left[\sum_{j=1}^{\infty} \sum_{i=1}^{S_R-1} \delta_{i+j,s} j n_j \frac{in_i}{g} + \sum_{j=1}^{\infty} \delta_{S_R+j,s} j n_j \left(1 - \sum_{i=1}^{S_R-1} \frac{in_i}{g}\right) - s n_s \right] \quad \text{for } s > S_R. \quad (4)$$

The first gain term on the R.H.S. of Eq. (2) comes from the merging process of two clusters of size i and j . One node is randomly selected from the set R , and the other is selected from all the nodes. The second loss term comes from the merging process of one cluster of size s and another cluster of any size. The last term, with the Kronecker delta, is contributed by an incoming isolated node at each time step. Note that when $s = S_R$, the loss term needs to take into account the fact that some clusters of size S_R can belong to the set R and others with the same size can belong to the set R^c . Thus, the second loss term appears in the form $p(1 - \sum_{k=1}^{S_R-1} \frac{k n_k}{g})$. When $s > S_R$, the loss term becomes simple because cluster loss occurs only when one node is selected from all the nodes. How-

ever, one needs to count the gain term carefully when one node is selected from a cluster of size S_R from the set R . We remark that to obtain the above derivation, we ignored the case in which two nodes are chosen from the same cluster. The reason is that this case contributes to the rate equations at a high order, $O(1/N^2)$. We confirm the validity of this approximation by comparing the solution of the rate equation with the result of numerical simulation later.

In the steady state, one may regard $S_R(p, t)$ and $n_s(p, t)$ as being time-independent. Then the L.H.S. of Eqs. (2)–(4) becomes $n_s(p)$ because $N(t) = t + 1$, and the rate equations are rewritten as follows:

$$n_s = p \left[\sum_{i,j=1}^{\infty} \frac{in_i j n_j}{g} \delta_{i+j,s} - \left(1 + \frac{1}{g}\right) s n_s \right] + \delta_{1s} \quad \text{for } s < S_R, \quad (5)$$

$$n_s = p \left[\sum_{i,j=1}^{\infty} \frac{in_i j n_j}{g} \delta_{i+j,s} - s n_s - \left(1 - \sum_{k=1}^{S_R-1} \frac{k n_k}{g}\right) \right] + \delta_{1s} \quad \text{for } s = S_R, \quad (6)$$

$$n_s = p \left[\sum_{j=1}^{\infty} \sum_{i=1}^{S_R-1} \delta_{i+j,s} j n_j \frac{in_i}{g} + \sum_{j=1}^{\infty} \delta_{S_R+j,s} j n_j \left(1 - \sum_{i=1}^{S_R-1} \frac{in_i}{g}\right) - s n_s \right] \quad \text{for } s > S_R. \quad (7)$$

IV. THE CLUSTER SIZE DISTRIBUTION $n_s(p)$

Here we solve the rate equation of $n_s(p)$ for a given g . First, when $s = 1$, the rate equation becomes $n_1 = -p(1 + \frac{1}{g})n_1 + 1$ for $S_R > 1$ and $n_1 = -p(n_1 + 1) + 1$ for $S_R = 1$. Thus, $n_1(p)$ becomes

$$n_1 = \begin{cases} \frac{1}{1+p(1+\frac{1}{g})} & S_R(p) > 1 \quad (p > p_1), \\ \frac{1-p}{1+p} & S_R(p) = 1 \quad (p < p_1). \end{cases} \quad (8)$$

The two solutions become the same at $p = (1-g)/(1+g)$, as shown in Fig. 3(b). This p is denoted as p_1 . For $g = 0.4$, $p_1 = 0.4285714 \dots$

Next, when $s = 2$, the rate equations are as follows: $n_2 = p[(n_1 n_1/g) - 2n_2(1 + 1/g)]$ for $S_R > 2$; $n_2 =$

$p[(n_1 n_1/g) - 2n_2 - (1 - n_1/g)]$ for $S_R = 2$; $n_2 = p(n_1 - 2n_2)$ for $S_R = 1$. We obtain n_2 as follows:

$$n_2 = \begin{cases} \frac{p \frac{n_1^2}{g}}{1+2p(1+\frac{1}{g})} & S_R > 2 \quad (p > p_2), \\ \frac{p[\frac{n_1^2}{g} - (1 - \frac{n_1}{g})]}{1+2p} & S_R = 2 \quad (p_1 < p < p_2), \\ \frac{p n_1}{1+2p} & S_R = 1 \quad (p < p_1). \end{cases} \quad (9)$$

Two kinks (crossovers) exist in $n_2(p)$, as shown in Fig. 3(c). The position p of the first kink is just p_1 , and that of the second kink is determined by setting n_2 for $S_R > 2$ equal to that for $S_R = 2$. This position is denoted as p_2 . For $g = 0.4$, $p_2 = 0.5653082 \dots$

In general, when $s > 1$, the cluster size distribution $n_s(p)$ can be obtained from the rate equations in the

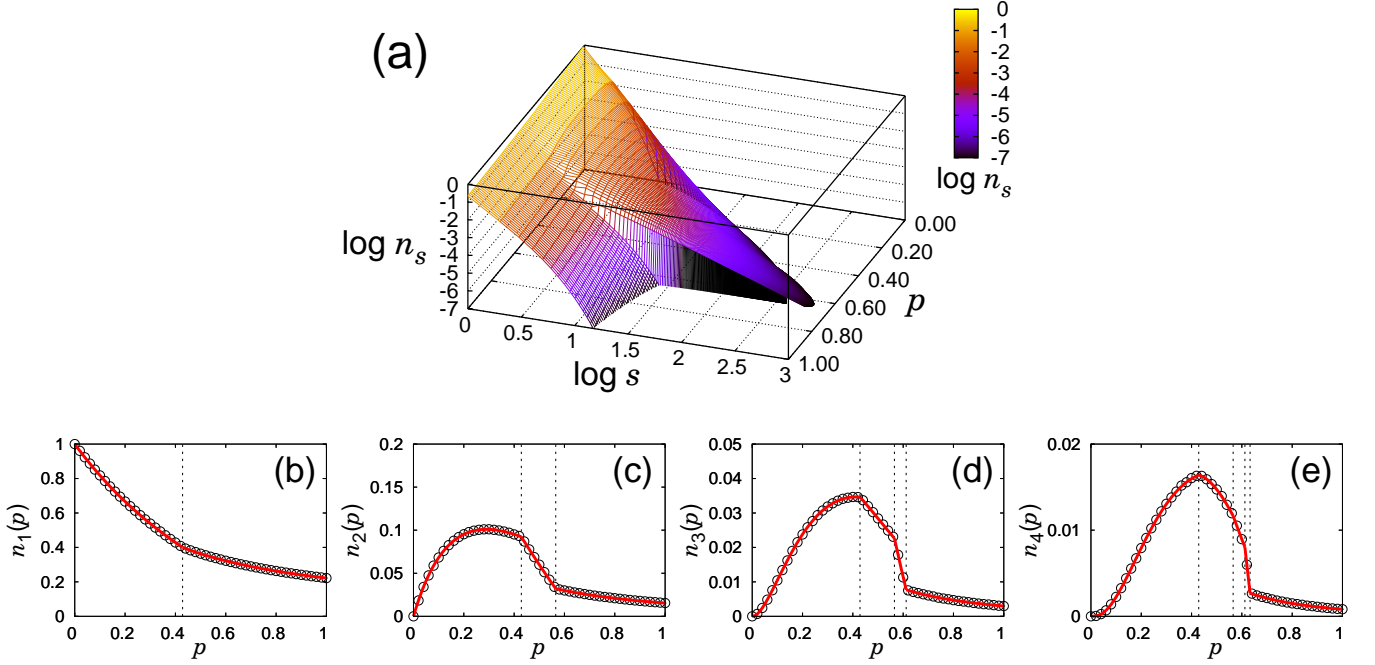


FIG. 3. Cluster size distribution $n_s(p)$ as a function of s and p . The system size $N = 10^6$ and $g = 0.4$ are taken. (a) Three-dimensional plot of $n_s(p)$ as a function of s and p . A clear discontinuous pattern exists. (b) Plot of $n_1(p)$ versus p . A crossover exists at p_1 . (c) Plot of $n_2(p)$ versus s . Two crossover behaviors occur at p_1 and p_2 , where $p_1 < p_2$. (d) $n_3(p)$, and (e) $n_4(p)$. Symbols represent simulation results, and solid lines are analytical results. Dotted vertical lines represent p_{S_R} for $S_R = 1, 2, 3$, and 4 at $p_{S_R=1} = 0.4285714$, $p_{S_R=2} = 0.5653082$, $p_{S_R=3} = 0.6120164$, and $p_{S_R=4} = 0.6327279$, which are close to the simulation results.

steady state as follows:

$$n_s(p) = \begin{cases} \frac{p \sum_{i,j=1}^{\infty} \frac{in_i j n_j}{g} \delta_{i+j,s} + \delta_{1s}}{1+sp(1+\frac{1}{g})} & s < S_R, \\ p \left[\frac{\sum_{i,j=1}^{\infty} \frac{in_i j n_j}{g} \delta_{i+j,s} - \left(1 - \sum_{k=1}^{S_R-1} \frac{kn_k}{g}\right) \right]}{1+sp} & s = S_R, \\ p \left[\frac{\sum_{j=1}^{\infty} \sum_{i=1}^{S_R-1} \delta_{i+j,s} j n_j \frac{in_i}{g} + \sum_{j=1}^{\infty} \delta_{S_R+j,s} j n_j \left(1 - \sum_{i=1}^{S_R-1} \frac{in_i}{g}\right) \right]}{1+sp} & s > S_R. \end{cases} \quad (10)$$

There exist s kinks on the curve n_s at p_1, \dots, p_s in ascending order of p . The position of the last kink p_s is determined by setting n_s for $S_R > s$ equal to n_s for $S_R = s$. For convenience, we use the index as S_R to avoid confusion with the index of cluster size s . The positions p_{S_R} as a function S_R are listed in Table I.

As shown in Fig. 3(b)-3(e), the interval between two successive crossover points becomes narrower with increasing S_R . The position p_{S_R} seems to converge to a certain value, p_{∞} , in a power-law form of $p_{\infty} - p_{S_R}$ as a function of S_R asymptotically as shown in Fig. 4. Here, p_{∞} is estimated to be $0.65948 \dots$.

V. TWO CRITICAL POINTS, p_b AND p_c

For a given p , $S_R(p)$ is determined as in Table I. Then one can obtain $n_s(p)$ as a function of s from the rate equations. Figures 5(a)-5(c) show the distributions n_s versus s for a given fixed p , which corresponds to the $(\log n_s, \log s)$ plane of the three-dimensional plot of $n_s(p)$ in Fig. 3(a).

From the behavior of $n_s(p)$, we find that there exist two points, say p_b and p_c , which characterize the following three distinct intervals on the line of p : i) For $p < p_b$, $n_s(p)$ follows the power law $n_s(p) \sim s^{-\tau}$ for $s > S_R$ with exponent $\tau > 3$, whereas it decays exponentially as a function of s for $s < S_R$. ii) For $p_b \leq p < p_c$, $n_s(p)$

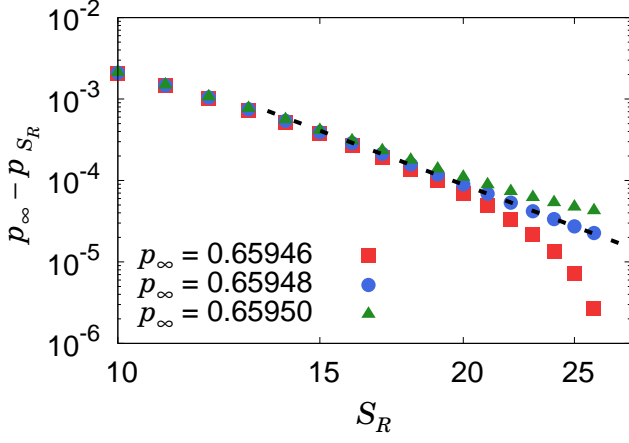


FIG. 4. Plot of $p_\infty - p_{S_R}$ versus S_R for $g = 0.4$. With the choice of $p_\infty = 0.65948$, a power-law behavior is obtained.

also follows a power law with exponent τ for $s > S_R$. Particularly, the exponent τ decreases continuously from $\tau = 3$ to 2 as p is increased from p_b to p_c . For $s < S_R$, $n_s(p)$ decays exponentially as a function of s . iii) For $p > p_c$, a giant cluster is generated and the distribution of the remaining finite clusters decays exponentially as a function of s .

The power-law behavior of $n_s(p)$ with $\tau > 3$ in the region i) is inherited from the infinite-order transition of the GRN model [8]. Thus the region i) is regarded as an

TABLE I. Values of p_{S_R} as a function of S_R for $g = 0.4$.

S_R	p_{S_R}
1	0.4285714285(1)
2	0.5653082407(1)
3	0.6120164684(1)
4	0.6327279058(1)
5	0.6433362667(1)
6	0.6492814220(1)
7	0.6528226406(1)
8	0.6550262003(1)
9	0.6564429142(1)
10	0.6573769871(1)
11	0.6580052394(1)
12	0.6584346536(1)
13	0.6587320681(1)
14	0.6589403439(1)
15	0.6590875632(1)
16	0.6591924579(1)
17	0.6592677124(1)
18	0.6593220275(1)
19	0.6593614370(1)
20	0.6593901656(1)
∞	0.6594712(1)

infinite-order critical region. Meanwhile, in the region ii), because $2 < \tau < 3$, the mean cluster size diverges. Thus the region ii) is regarded as a second-order critical region. It is noteworthy that while the critical behavior occurs at a critical point in a prototypical second-order transition, here it occurs in the region ii). At p_c^- , $\tau = 2$. This means that clusters are extremely heterogeneous and further suppression of the largest cluster leads to a discontinuous transition. This feature will be discussed later in the final section. Indeed, a discontinuous transition occurs at p_c . Both transition points for different g values are listed in Table II.

To determine p_b and p_c , here we introduce the generating function $f(x)$ of the probability sn_s that a randomly chosen node belongs to the cluster of size s , defined as

$$f(x) \equiv \sum_{s=1}^{\infty} sn_s x^s, \quad (11)$$

where x is the fugacity in the interval $0 < x < 1$. The giant cluster size G is obtained as $G = 1 - \sum_{s=1}^{\infty} sn_s = 1 - f(1)$. The mean cluster size is obtained as $\langle s \rangle = \sum_{s=1}^{\infty} s^2 n_s = f'(1)$, where the prime represents the derivative with respect to x . To determine p_b (p_c), we consider the case of S_R being finite (infinite).

A. For finite S_R

When S_R is finite, we derive the recurrence relation for n_s . First, when $S_R = 1$, the rate equations in the steady state are simply reduced as follows:

$$n_1 = -p(n_1 + 1) + 1, \quad (12)$$

$$n_s = p[(s-1)n_{s-1} - sn_s], \quad \text{for } s > 1. \quad (13)$$

Then, one can obtain the generating function $f(x)$ as

$$f(x) = -xp f'(x) - px + x + px^2 f'(x) + px f(x). \quad (14)$$

The giant cluster size G is $G = 1 - \sum_{s=1}^{\infty} sn_s = 1 - f(1) = 0$. The mean cluster size is obtained as $\langle s \rangle = \sum_{s=1}^{\infty} s^2 n_s = f'(1) = 1/(1-2p)$. So the mean cluster size diverges at $p_b = 1/2$. If this value is larger than p_1 for a given g , then we move to $S_R = 2$.

When $S_R = 2$, $G = 0$ and $\langle s \rangle = f'(1) = 1/[1-4p+(2pn_1/g)]$. Generally, for finite S_R , $f(1)$ is one, and $\langle s \rangle$ can be derived as

$$\langle s \rangle^{-1} = \left[1 + 2p \left(\sum_{i=1}^{S_R-1} \frac{(S_R-i)n_i}{g} - S_R \right) \right]. \quad (15)$$

To obtain p_b , once we set $S_R = 1$ and check whether there exists a certain value of p less than p_{S_R} , say p_* , such that $\langle s \rangle^{-1} = 0$. If the solution exists, p_* is a critical point p_b and S_R is the size of the largest cluster in the set R . Otherwise, we increase S_R by one, and try to find

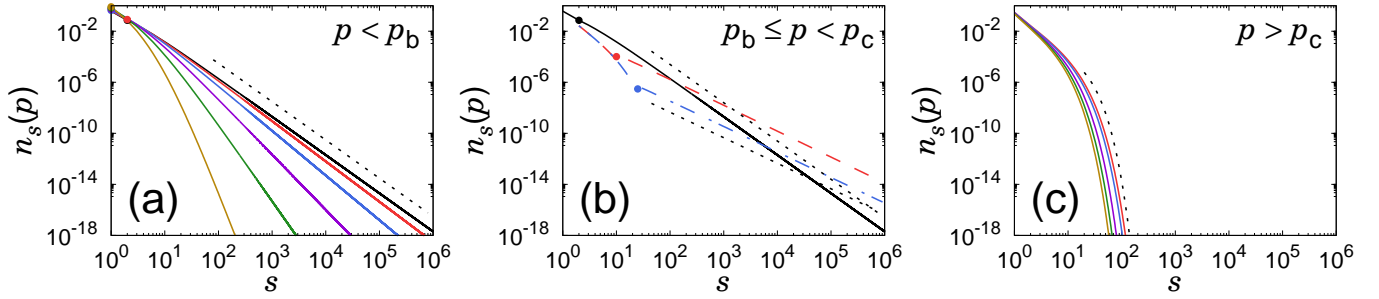


FIG. 5. Plots of the cluster size distribution $n_s(p)$ versus s for a given p and $g = 0.4$. Three cases of $n_s(p)$ are distinguished: (a) For $p < p_b$, $n_s(p)$ asymptotically follows the power law $\sim s^{-\tau}$ with $\tau > 3$. The slope of the dotted guide line is -3 . Solid lines are obtained for $p = 0.472576 \approx p_b$, 0.45, 0.4, 0.3, 0.2, and 0.1 from right to left. (b) For $p_b \leq p < p_c$, in the small-cluster-size region, $n_s(p)$ decays exponentially and then exhibits power-law behavior with $2 < \tau \leq 3$. Solid, dashed, and dashed-dotted lines represent p_{S_R} , where $S_R = 2, 10$ and 25 , respectively. Two dotted lines are guide lines with slopes of -2 and -3 . (c) For $p \geq p_c$, $n_s(p)$ for finite clusters shows exponentially decaying distributions. Solid curves represent $p = 0.6596, 0.7, 0.8, 0.9$, and 1.0 from right to left. Dotted curve is an exponentially decaying guide curve.

TABLE II. Numerical estimates of the transition points p_b and p_c . The critical exponents τ are calculated at $p = p_b$ and p_c for $g = 0.1 - 0.9$. We note that the exponent τ at p_c becomes difficult to obtain as g approaches one.

g	p_b	p_c	ΔG	$\tau(p_b)$	$\tau(p_c)$
0.1	1/2	0.905(1)	0.900(1)	3.00(1)	2.00(1)
0.2	1/2	0.817(1)	0.800(1)	3.00(1)	2.00(1)
0.3	1/2	0.736(1)	0.700(1)	3.00(1)	2.00(1)
1/3	1/2	0.710(1)	0.666(1)	3.00(1)	2.00(1)
0.4	0.473(1)	0.660(1)	0.600(1)	3.00(1)	2.00(1)
0.5	0.440(1)	0.587(1)	0.500(1)	3.00(1)	2.00(1)
0.6	0.405(1)	0.516(1)	0.400(1)	3.00(1)	2.00(1)
0.7	0.367(1)	0.447(1)	0.300(1)	3.00(1)	1.99(1)
0.8	0.323(1)	0.376(1)	0.200(1)	3.00(1)	1.99(1)
0.9	0.268(1)	0.297(1)	0.100(1)	3.00(1)	1.8(2)
1.0	1/8	1/8	0	3	-

a solution satisfying $\langle s \rangle^{-1} = 0$. We repeat these steps until the solution is found. The obtained values p_b for different g are listed in Table II.

This formula implies that even though the order parameter $G(p)$ is zero for $p < p_c$, the mean cluster size $\langle s \rangle$ can diverge at a certain p_b less than p_c .

B. For infinite S_R

We consider the limit $S_R(p) = \infty$, which corresponds to the case $p > p_\infty$. In this case, the rate equation (5) is valid for all cluster sizes s . Equations (5)–(7) reduce to

the following two equations:

$$n_1 = \frac{1}{1 + (1 + \frac{1}{g})p}, \quad (16)$$

$$n_s = \frac{p}{1 + (1 + \frac{1}{g})sp} \sum_{j=1}^{s-1} \frac{j(s-j)n_j n_{s-j}}{g}, \quad (17)$$

where s is limited to finite clusters. The generating function associated with sn_s satisfies the following relation:

$$f(x) = -x(1 + \frac{1}{g})pf'(x) + \frac{2}{g}pxf(x)f'(x) + x, \quad (18)$$

and in another form,

$$f'(x) = \frac{1 - \frac{f(x)}{x}}{(1 + \frac{1}{g}) - \frac{2}{g}f(x)} \frac{1}{p}. \quad (19)$$

Performing numerical integration, we obtain $f(1)$ and $f'(1)$, which correspond to the order parameter $G(p)$ and $\langle s \rangle$ for given p and g in the region $p \geq p_\infty$. At p_∞ , this order parameter value $G(p_\infty)$ is not zero but finite, indicating that the transition at p_∞ is first-order. Moreover, $G(p_\infty)$ represents the jump size of the order parameter ΔG of the discontinuous transition. We obtain the cluster size distribution using the formula (10), which follows a power law with $\tau \simeq 2$. Therefore, we think that $p_\infty = p_c$. The results for G and $1/\langle s \rangle$ in the entire region p are shown in Fig. 6 for $g = 0.2, 0.4$, and 0.6 . Numerical data of p_b , p_c , ΔG , $\tau(p_b)$, and $\tau(p_c)$ for different g are listed in Table II. Indeed, the order parameters are discontinuous at p_c for different $g < 1$. We draw a phase diagram shown in Fig. 7 in the plane of (p, g) .

VI. THE p DEPENDENCE OF τ IN THE CRITICAL REGION

When $p < p_c$, the cluster size distribution follows a power law with exponent τ . This exponent τ depends

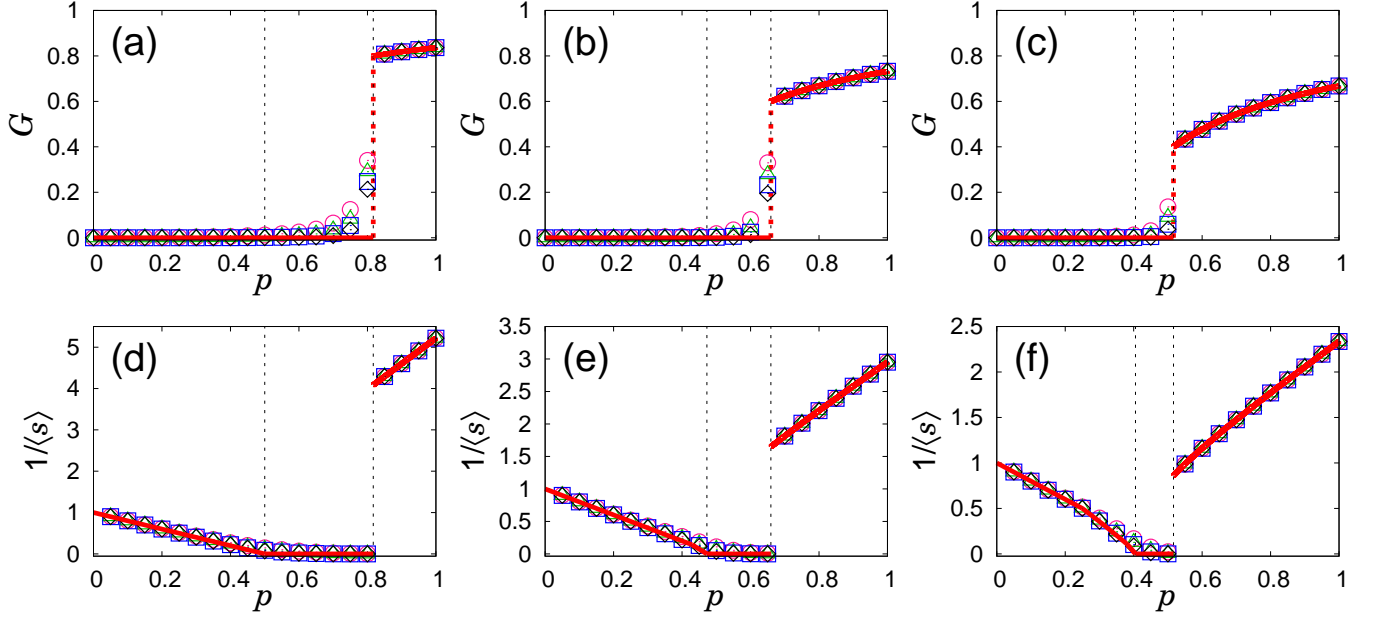


FIG. 6. Plot of G and $1/\langle s \rangle$ as a function of p for $g = 0.2$ in (a) and (d), 0.4 in (b) and (e), and 0.6 in (c) and (f), respectively. Symbols represent the simulation results for $N = 10^4$ (\circ), 10^5 (\triangle), 10^6 (\square), and 10^7 (\diamond). Each data point was averaged over 10^3 times. The solid (red) lines are calculated from $f(1)$ and $f'(1)$ for G and $\langle s \rangle$, respectively. The two vertical dotted lines represent p_b and p_c .

on the link occupation probability p . Here we derive $\tau(p)$ explicitly for $g \rightarrow 0$ and $S_R = 1$. In this case, cluster merging dynamics occurs only between isolated nodes and another cluster of any size. From Eq. (10),

one can obtain the explicit form of $n_s(p)$ as follows:

$$n_s(p) = \frac{(s-1)! p^{s-1} n_1(p)}{(1+sp)(1+(s-1)p) \cdots (1+2p)}, \quad (20)$$

where $n_1(p)$ is $(1-p)/(1+p)$, and $S_R = 1$. Using the Stirling formula, the gamma function $\Gamma(z) = (z-1)!$ is

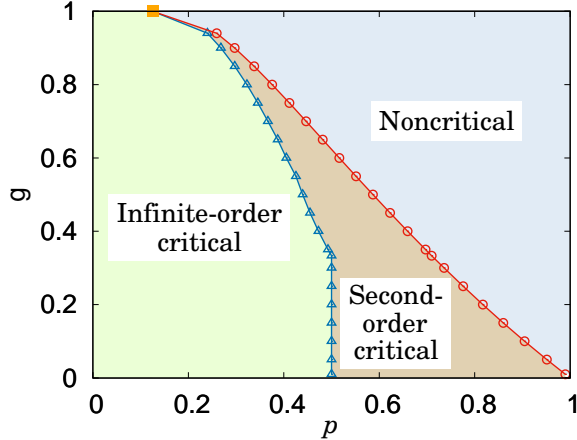


FIG. 7. Two critical points p_b and p_c for various g . Symbols \triangle and \circ represent p_b and p_c . $n_s(p)$ decays following a power law with $\tau > 3$ in the infinite-order critical region and $2 < \tau < 3$ in the second-order critical region. Thus, the mean cluster size is finite and diverges, respectively. As g approaches one, the two critical points are closer and converge to the critical point of an infinite-order phase transition, represented by \blacksquare .

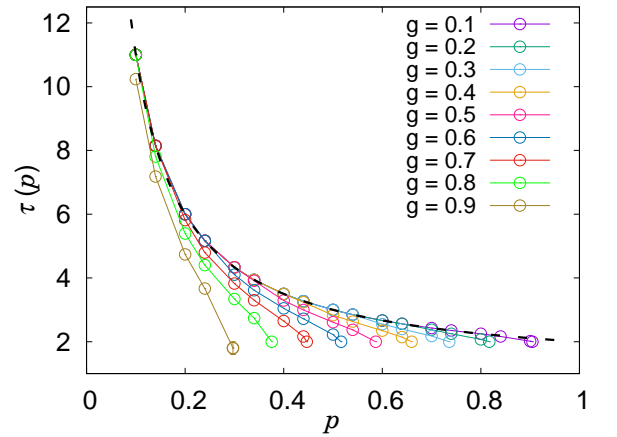


FIG. 8. Plot of τ versus p for different g . τ becomes two as p approaches p_c for any g . The black dashed curve is a guide curve representing $1 + 1/p$, which is obtained from the case $S_R = 1$.

rewritten as

$$\Gamma(z) \sim z^{z-\frac{1}{2}} e^{-z} \sqrt{2\pi} \left(1 + \frac{1}{12z} + \frac{1}{288z^2} - \frac{139}{51840z^3} - \frac{571}{2488320z^4} \right) \text{ as } |z| \rightarrow \infty.$$

Using this formula, one can obtain the asymptotic behavior of Eq. (20) as

$$n_s(p) = \frac{\Gamma(s)\Gamma(\frac{1}{p}+2)}{\Gamma(s+\frac{1}{p}+1)} n_1(p) \sim s^{-(\frac{1}{p}+1)}, \quad (21)$$

where the critical exponent $\tau = \frac{1}{p} + 1$, which is independent of g . Figure 8 shows τ as a function of p . Because the merging dynamics starts from $S_R = 1$, $\tau = 1 + 1/p$ appears in the envelope of $\tau(p)$.

VII. DISCUSSION AND SUMMARY

The restricted growing random network (r -GRN) model was built based on the restricted Erdős-Rényi (r -ER) model recently introduced in Ref. [25]. This r -ER model is a static network model, containing N nodes all the times. The two-node selection rule for a link connection is the same as that of the r -GRN model but once the two nodes are selected at time step t , they are connected definitely. This model contains a global suppression dynamics. In this r -ER model, a power-law behavior of $n_s(t_c)$ without any exponential cutoff appears only at the point t_c^+ just after the order parameter jumps. The exponent τ is in the range $2 \leq \tau \leq 3$ depending on the parameter g . Thus, the model exhibits not only a discontinuous transition but also a critical behavior. The critical behavior appears in the region where the order parameter is finite. Contrary to the transition behavior of this r -ER static network model, the critical behavior in the r -GRN model appears below the transition point p_c , so that the order parameter still remains zero.

For the r -GRN model, the power-law decay of $n_s(p)$ appears in a steady state over all cluster sizes without forming any bump or exponential cutoff even for all $p < p_c$. This reason is as follows: At each time step, a new node is added and remains as an isolated with the probability $1 - O(1/N)$, which is close to unity as N becomes large. Thus, single-size nodes are accumulated in the system and they are more likely to merge finite-size clusters, reducing the frequency of merging two large clusters. When dynamics reaches a steady state, the cluster merging dynamics self-organizes and forms a power-law behavior of $n_s(p)$. We considered an extreme case that the new node tries to merge a finite-size cluster at every time step and it merges successfully with the probability p . In this case, $n_s(p)$ is obtained as $\sim s^{-(1+1/p)}$ in Eq. (21). More generally, as p is increased, more links are added, and the largest cluster becomes larger, and thus the exponent $\tau(p)$ is continuously decreasing. Because the transition point is delayed by the suppression effect,

τ can decrease down to two. This eventually leads to a discontinuous PT, because the largest cluster size scales as $N(t)^{1/(\tau-1)}$, where $N(t)$ denotes the system size at a certain time t in steady state, and it reaches up to the extensive size to the system size when $\tau = 2$ regardless t in the steady state.

This tricritical-like behavior at $\tau = 2$ can be seen in the classical polymer aggregation model [27–29]. The cluster aggregation phenomena in a static system were described via the rate equation,

$$\frac{dn_s(t)}{dt} = \sum_{i+j=s} \frac{w_i n_i}{c(t)} \frac{w_j n_j}{c(t)} - 2 \frac{w_s n_s}{c(t)} \sum_{i=1} \frac{w_i n_i}{c(t)}, \quad (22)$$

where $c(t) = \sum_s w_s n_s(t)$. The first term on the R.H.S. represents the aggregation of two clusters of sizes i and j with $i + j = s$, and the second term is for a cluster of size s merging with another cluster of any size. The rate equation reduces to the ER network model when $c(t) = 1$, which occurs when $w_i = i$. A general case, $w_i = i^\omega$, was studied [27–29] long ago. In this case, as ω is smaller, the growth of large clusters is more suppressed. When $1/2 < \omega < 1$, a continuous transition occurs at t_c ; a giant cluster is generated for $t > t_c$. At $t = t_c$, the cluster size distribution follows a power law with exponent $\tau = \omega + (3/2)$. When $0 < \omega \leq 1/2$, a discontinuous transition occurs, and the exponent $\tau = 1 + 2\omega$. The case $\omega = 1/2$, for which $\tau = 2$, is marginal for a second-order and a first-order transition. We remark that another model recent introduced also generates either a continuous or a discontinuous PT by controlling the suppression strength similar to the above case [30]. These two cases are all for static networks. Even though the system type and the underlying mechanism of static and growing networks are different, on the basis of the above result, we could confirm that the discontinuous transition at p_c is induced by the increase of the cluster size heterogeneity across the point with $\tau = 2$.

The BKT transition was found originally in the two-dimensional XY model in thermal systems [1–5]. The origin of the BKT transition in thermal systems is different from that of the percolation model, but there exist some similarities or dissimilarity in the transition behavior: In the XY model, the singular part of the free energy behaves as $f(t) \sim \exp(-bt^{-1/2})$ with a positive constant b for the reduced temperature $t = (T - T_c)/T_c > 0$, similar to the order parameter $G(p)$ for $p > p_c$ in Eq. (1). The correlation function decays in a power-law manner as $\Gamma(r) \sim r^{-\eta(T)}$ for $t < 0$, where $\eta(T) \sim T$ is continuously varying depending on T . This is often called the quasi-long-range order. In a second-order transition $\Gamma(r) \sim r^{-\eta} \exp(-r/\xi)$ for $t < 0$. In this regard, the pure power-law behavior of $\Gamma(r)$ in the infinite-order transition implies $\xi = \infty$ for $t < 0$. Indeed, $\xi = \infty$ for $t < 0$ in the XY model. The continuous varying exponent $\eta(T)$ in the XY model corresponds to the exponent $\tau(p)$ of the cluster size distribution $n_s(p) \sim s^{-\tau(p)}$. In a second-order PT, $n_s \sim s^{-\tau} \exp(-s/s^*)$ for $p < p_c$, where s^* is a characteristic cluster size in the region $p < p_c$. Again, the

pure power-law behavior of the infinite-order PT implies that $s^* = \infty$ for $p < p_c$. The susceptibility is obtained using the thermodynamic relation, $\chi \sim \int d^2r \Gamma(r)$. One can find that χ diverges for $\eta < 2$, while it is finite for $\eta > 2$. Because η increases with temperature, χ diverges for $t < 0$ and finite for $t > 0$, where the critical temperature is determined by $\eta = 2$. In percolation, the susceptibility $\chi = \sum_s s^2 n_s$ diverges for $\tau < 3$, while it is finite for $\tau > 3$. For the GRN model, $\tau > 3$ for $p < p_c$. Thus, the susceptibility is finite for $p < p_c$. For $p > p_c$, n_s of finite clusters decays exponentially. Thus the susceptibilities on both sides of a transition point are finite. Even though the order parameter behaves as an infinite-order transition, the susceptibility behavior differently from that of the XY model. On the other hand, for the r -GRN model, the susceptibility diverges in one side and is finite in the other side, similar to those of the XY model.

The BKT transition can occur even in static networks. For instance, the percolation model in one-dimension with $1/r^2$ long-range connections [20] and on hierarchical networks with short-range and long-range connections [31] exhibit BKT infinite-order PTs. As future works, it would be interesting to check whether the diverse phases and phase transitions we obtained occur or not in those static network models when the suppression rule is applied. Moreover, in our study, the suppression rule is applied to large clusters, because the giant cluster size per node is the order parameter in percolation problem. As an extension of our work to thermal systems, it would be interesting to find an essential quantity of thermal BKT systems, for instance, the formation of spin waves or vortices, and see if we can control the BKT transition by the suppression effect. The pattern formation by topological defects in active liquid crystals recently draws considerable attention [33, 34]. Various patterns generated in that system are governed basically by the BKT theory. It would be interesting to note how those patterns are changed when the system is applied by a certain suppression effect.

In summary, we have investigated how a BKT PT of growing networks is changed when the growth of large

clusters in the system is suppressed. We introduced the r -GRN model, modified from the GRN model by including the suppression rule. In the r -GRN model, we found that there exist two transition points, p_b and p_c , and three phases. i) In the region $p < p_b$, the order parameter is zero, and the cluster size distribution decays according to a power law without any exponential cutoff and with exponent $\tau(p)$ larger than three. Thus, the mean cluster size is finite. The exponent $\tau(p)$ continuously decreases as p is increased. Accordingly, the region $p < p_b$ is regarded as an infinite-order type critical region. ii) For the region $p_b < p < p_c$, we found that the order parameter is zero, and the cluster size distribution follows a power law without any exponential cutoff, where the exponent $\tau(p)$ ranges between two and three. Thus, the mean cluster size diverges. This behavior is reminiscent of the critical behavior occurring at the critical point of a second-order transition. Thus, region ii) is regarded as a second-order type critical region. The fact that the mean cluster size diverges, even though the largest cluster has not grown to the extensive size yet, implies that the fluctuations of subextensive-finite clusters diverge preceding to the emergence of the giant cluster of extensive size. Similar behavior occurs in a hierarchical model [32]. iii) At p_c , a discontinuous transition occurs. iv) The region $p > p_c$ is regarded as a noncritical region because the order parameter is finite, and the cluster size distribution decay exponentially. Thus, our model contains the three regimes of the infinite-order, second-order, and first-order transitions. We obtained various properties of the transition behaviors analytically and numerically.

ACKNOWLEDGMENTS

This work was supported by the National Research Foundation of Korea (NRF) through Grant Nos. NRF-2014R1A3A2069005 (BK) and NRF-2017R1D1A1B03032864 (SWS), and a TJ Park Science Fellowship from the POSCO TJ Park Foundation (SWS).

-
- [1] V. L. Berezinskii, *Destruction of Long-range Order in One-dimensional and Two-dimensional Systems Having a Continuous Symmetry Group I. Classical Systems*, Sov. Phys. JETP **32**, 493 (1971).
 - [2] V. L. Berezinskii, *Destruction of Long-range Order in One-dimensional and Two-dimensional Systems Possessing a Continuous Symmetry Group II. Quantum Systems*, Sov. Phys. JETP **34**, 601 (1972).
 - [3] J. M. Kosterlitz and D. J. Thouless, *Long Range Order and Metastability in Two Dimensional Solids and Superfluids*, J. Phys. C **5**, L124 (1972).
 - [4] J. M. Kosterlitz and D. J. Thouless, *Ordering, metastability and phase transitions in two-dimensional systems*, J. Phys. C **6**, 1181 (1973).
 - [5] J. M. Kosterlitz, *The Critical Properties of the Two-Dimensional XY Model*, J. Phys. C **7**, 1046 (1974).
 - [6] J. M. Kosterlitz, *Nobel Lecture: Topological Defects and Phase Transitions*, Rev. Mod. Phys. **89**, 040501 (2017).
 - [7] F. Duncan M. Haldane, *Nobel Lecture: Topological Quantum Matter*, Rev. Mod. Phys. **89**, 040502 (2017).
 - [8] D. S. Callaway, J. E. Hopcroft, J. M. Kleinberg, M. E. J. Newman, and S. H. Strogatz, *Are Randomly Grown Graphs Really Random?*, Phys. Rev. E **64**, 041902 (2001).
 - [9] S. N. Dorogovtsev, J. F. F. Mendes, and A. N. Samukhin, *Anomalous Percolation Properties of Growing Networks*, Phys. Rev. E **64**, 066110 (2001).
 - [10] M. E. Newman, *Coauthorship networks and patterns of scientific collaboration*, Proc Natl. Acad. Sci. USA **101**,

- 5200 (2004).
- [11] D. Lee, K.-I. Goh, B. Kahng, and D. Kim, *Complete Trails of Coauthorship Network Evolution*, Phys. Rev. E **82**, 026112 (2010).
 - [12] J. Leskovec, J. Kleinberg, and C. Faloutsos, *Graph Evolution: Densification and Shrinking Diameters*, ACM Trans. Knowl. Disc. Data **1**, 2 (2007).
 - [13] R. V. Solé, R. Pastor-Satorras, E. D. Smith, and T. Kepler, *A model of Large-Scale Proteome Evolution*, Adv. Complex Syst. **05**, 43 (2002).
 - [14] A. Vázquez, A. Flammini, A. Maritan, and A. Vespignani, *Modeling of Protein Interaction Networks*, ComplexUs **1**, 38 (2003).
 - [15] J. Kim, P. L. Krapivsky, B. Kahng, and S. Redner, *Infinite-Order Percolation and Giant Fluctuations in a Protein Interaction Network*, Phys. Rev. E **66**, 055101 (2002).
 - [16] G. Jaeger, *The Ehrenfest classification of phase transitions: Introduction and evolution*, Arch Hist Exact Sci **53**, 5181 (1998).
 - [17] S. M. Oh, S.-W. Son, and B. Kahng, *Explosive Percolation Transitions in Growing Networks*, Phys. Rev. E **93**, 032316 (2016).
 - [18] D. Stauffer and A. Aharony, *Introduction to Percolation Theory* (Taylor and Francis, London, 1994).
 - [19] R. Cohen, K. Erez, D. ben-Avraham, and S. Havlin, *Resilience of the Internet to Random Breakdowns*, Phys. Rev. Lett. **85**, 4626 (2000).
 - [20] P. Grassberger, *SIR Epidemics with Long-Range Infection in One Dimension*, J. Stat. Mech. P04004 (2013).
 - [21] O. Riordan and L. Warnke, *Explosive Percolation Is Continuous*, Science **333**, 322 (2011).
 - [22] Y. S. Cho, S. Hwang, H. J. Herrmann, and B. Kahng, *Avoiding a Spanning Cluster in Percolation Models*, Science **339**, 1185 (2013).
 - [23] P. Erdős and A. Rényi, *On the Evolution of Random Graphs*, Publ. Math. Inst. Hungar. Acad. Sci. A **5**, 17 (1960).
 - [24] K. Panagiotou, R. Sphöel, A. Steger, and H. Thomas, *Explosive Percolation in Erdős-Rényi-like Random Graph Processes*, Electron. Notes Discrete Math. **38**, 699 (2011).
 - [25] Y. S. Cho, J. S. Lee, H. J. Herrmann, and B. Kahng, *Hybrid Percolation Transition in Cluster Merging Processes: Continuously Varying Exponents*, Phys. Rev. Lett. **116**, 025701 (2016).
 - [26] K. Choi, D. Lee, Y. S. Cho, J. C. Thiele, H. J. Herrmann, and B. Kahng, *Critical phenomena of a hybrid phase transition in cluster merging dynamics*, Phys. Rev. E **96**, 042148 (2017).
 - [27] R. M. Ziff, E. M. Hendriks, and M. H. Ernst, *Critical Properties for Gelation: A Kinetic Approach*, Phys. Rev. Lett. **49**, 593 (1982).
 - [28] F. Levyraz and H. R. Tschudi, *Singularities in the Kinetics of Coagulation Processes*, J. Phys. A **14**, 3389 (1981).
 - [29] Y. S. Cho, B. Kahng, and D. Kim, *Cluster Aggregation Model for Discontinuous Percolation Transitions*, Phys. Rev. E **81**, 030103 (2010).
 - [30] G. Bianconi, *Rare Events and Discontinuous Percolation Transitions*, Phys. Rev. E **97**, 022314 (2018).
 - [31] A. N. Berker, M. Hinczewski, and R. R. Netz, *Critical Percolation Phase and Thermal Berezinskii-Kosterlitz-Thouless Transition in a Scale-Free Network with Short-Range and Long-Range Random Bonds*, Phys. Rev. E **80**, 041118 (2009).
 - [32] S. Boettcher, V. Singh, and M. R. Ziff, *Ordinary Percolation with Discontinuous Transitions*, Nat. Commun. **3**, 787 (2012).
 - [33] M. C. Marchetti, et al., *Hydrodynamics of Soft Active Matter*, Rev. Mod. Phys. **85**, 1143 (2013).
 - [34] X. Tang and J. Selinger, *Orientation of Topological Defects in 2D Nematic Liquid Crystals*, Soft Matter **13**, 5481 (2017).